IOPscience iopscience.iop.org

Home Search Collections Journals About Contact us My IOPscience

Rise-Time Elongation Effects on Trapped Field and Temperature Rise in Pulse Field Magnetization for High Temperature Superconducting Bulk

This content has been downloaded from IOPscience. Please scroll down to see the full text.

2005 Jpn. J. Appl. Phys. 44 4919

(http://iopscience.iop.org/1347-4065/44/7R/4919)

View the table of contents for this issue, or go to the journal homepage for more

Download details:

IP Address: 160.29.75.151
This content was downloaded on 06/06/2017 at 08:48

Please note that terms and conditions apply.

You may also be interested in:

Magnetic pulse cleaning of products
V P Smolentsev, S V Safonov, E V Smolentsev et al.

Trapped Field over 4 Tesla on GdBaCuO Bulk by Pulse Field Method and Magnetizing Mechanism
Hiroyuki Fujishiro, Masahiko Kaneyama, Tatsuya Tateiwa et al.

Simulation of temperature and magnetic field distribution in superconducting bulk duringpulsed field magnetization
Hiroyuki Fujishiro and Tomoyuki Naito

Enhancement of trapped field and total trapped flux on GdBaCuO bulk by theMMPSC+IMRA method
Hiroyuki Fujishiro, Takuya Hiyama, Tomoyuki Naito et al.

Enhancement of Trapped Field and Total Trapped Flux on High Temperature Bulk Superconductor by a New Pulse-Field Magnetization Method
Hiroyuki Fujishiro, Tatsuya Tateiwa and Takuya Hiyama

Heat propagation analysis in HTSC bulks during pulse field magnetization
Hiroyuki Fujishiro, Shusuke Kawaguchi, Masahiko Kaneyama et al.

Temperature rise in an SmBaCuO after applying iterative pulse fields
Hiroyuki Fujishiro, Kazuya Yokoyama, Tetsuo Oka et al.

Mechanism of magnetic flux trapping on superconducting bulk magnetized by pulsed fieldusing a vortex-type coil
Hiroyuki Fujishiro, Tomoyuki Naito and Mitsuru Oyama

Japanese Journal of Applied Physics
Vol. 44, No. 7A, 2005, pp. 4919–4925
©2005 The Japan Society of Applied Physics

Rise-Time Elongation Effects on Trapped Field and Temperature Rise in Pulse Field Magnetization for High Temperature Superconducting Bulk

Hiroyuki FUJISHIRO*, Masahiko KANEYAMA, Kazuya YOKOYAMA[1], Tetsuo OKA[2] and Koshichi NOTO

Faculty of Engineering, Iwate University, 4-3-5 Ueda, Morioka 020-8551, Japan
[1]*National Institute for Materials Science, 3-13 Sakura, Tsukuba, Ibaraki 305-0003, Japan*
[2]*IMRA Material R&D Co., Ltd., 5-50 Hachiken-cho, Kariya, Aichi 448-0021, Japan*

(Received February 3, 2005; accepted April 8, 2005; published July 8, 2005)

Pulse field magnetization (PFM) using a magnetic pulse of $B_{ex} = 3.83$–5.53 T with various rise times t_r (= 6–20 ms) has been performed for the cryocooled SmBaCuO bulk superconductor starting at the initial temperature of 40 K. The time evolutions of temperature $T(t)$ and local field $B_L^P(t)$ have been measured on the bulk surface after applying the magnetic pulse. With increasing t_r, the temperature rise ΔT and the trapped field B_T^P increase for $B_{ex} \leq 4.70$ T and decrease for $B_{ex} = 5.53$ T. The rise time t_r required to realize the optimum B_T^P has been found to become longer for a smaller pulse field B_{ex}. From the analyses of the generated heat Q after five successive applications of pulses (Nos. 1–5) with the same amplitude, the Q(No. 5) value, which can be regarded as the viscous loss Q_v, decreases with increasing t_r, due mainly to the decrease in the flux propagation velocity v in the bulk with longer t_r. [DOI: 10.1143/JJAP.44.4919]

KEYWORDS: bulk superconductor, pulse field magnetization, rise time, temperature measurement, heat generation, pinning loss, viscous loss

1. Introduction

The practical application of high-T_c bulk superconductors as a high-strength bulk magnet has been attempted for a magnetic separation system to purify waste water[1] and for a magnetron sputtering apparatus,[2] for example. Static field-cooled magnetization (FCM) is usually applied to magnetize the high-T_c bulks, which can realize a high trapped field corresponding to the maximum trapping ability of magnetic field. Recently, the pulse field magnetization (PFM) technique has been intensively investigated and applied because of its relatively compact, inexpensive and mobile setup. The trapped field B_T^P and total trapped flux Φ_T^P induced by PFM are, however, generally smaller than those attained by FCM at low temperatures below 77 K. This is possibly the result of the large temperature rise ΔT due to the dynamical motion of the magnetic fluxes against the vortex pinning force F_p and the viscous force F_v. In order to enhance B_T^P and Φ_T^P induced by PFM, ΔT reduction is essential. Several approaches have been attempted, such as an iteratively magnetizing pulsed-field method with reduced amplitude (IMRA)[3] and a multi pulse technique with step wise cooling (MPSC).[4] We proposed to set a metal ring onto the bulk disk for ΔT reduction.[5] The B_T^P and Φ_T^P values were enhanced 10–20% with the presence of a stainless-steel ring because of the transfer of heat generated in the peripheral region of the bulk into the ring. Not only the strength of magnetic pulse B_{ex} but also the shape of the pulse, such as the rise time and pulse duration, must be taken into consideration to analyze the PFM process.

The amount of heat generated Q during PFM is considered to be given by the sum of the pinning loss Q_p and the viscous loss Q_v, where Q_v is proportional to the flux propagation velocity v. Thus the reduction of v in the bulk is a possible approach to reducing heat generation. Yanagi and coworkers measured the v value in SmBaCuO and YBaCuO bulks by the pick-up coil technique and estimated the pinning and viscous losses.[6,7] It is expected that v becomes faster with shorter rise time t_r of the magnetic pulse. Itoh *et al.* performed PFM at 77 K with $t_r = 1.3$ and 3.6 ms with the same B_{ex} and measured the total magnetic flux Φ_T^P.[8] However, no difference in Φ_T^P was observed in this range of t_r. We studied the time evolution and spatial distribution of the temperature rise $\Delta T(t)$ on the surface of cryocooled YBaCuO,[9,10] SmBaCuO[11,12] and GdBaCuO[10] bulks during PFM, where t_r was fixed at 12 ms. The $\Delta T(t)$ behavior changed depending on the initial bulk temperature T_s, the strength of the pulse field B_{ex} and the trapped field distribution before the application of magnetic pulse. We also estimated the total generated heat Q using the maximum ΔT based on the specific heat C of the bulk. By analyzing the pulse number dependence of Q for successive applications of pulses with a fixed amplitude B_{ex}, the contributions of Q_p and Q_v to the total Q were separated.[10] Q_p could be precisely estimated from the hysteresis loop of magnetization M vs applied field $\mu_0 H_a$, and Q_v was determined by subtracting the pinning loss $Q_p(MH)$, estimated from the M–$\mu_0 H_a$ hysteresis loop, from the total Q obtained in temperature measurements.[13]

In this paper, we investigate the time dependences of $T(t)$ and the local field $B_L^P(t)$ and the trapped field B_T^P [$= B_L^P$ (infinity)] on the surface of the cryocooled SmBaCuO bulk superconductor during successive applications of magnetic pulses of the same strength. We estimate the Q_p and Q_v values and discuss the t_r dependences of these values. We also discuss the possibility of B_T^P enhancement from the viewpoint of t_r dependence.

2. Experimental

A SmBaCuO bulk superconductor (Sm-bulk) of a disk shape (45 mm in diameter and 18 mm in thickness) with a highly c-axis-oriented structure was used. (fabricated by Dowa Mining Co., Ltd.) which consisted of 4 growth sector regions (GSR1-GSR4). The bulk crystal was composed of $SmBa_2Cu_3O_y$ (Sm123) and Sm_2BaCuO_5 (Sm211) with the molar ratio of Sm123 : Sm211 = 1.0 : 0.3, 15.0 wt% Ag_2O powder and 0.5 wt% Pt powder. The bulk was uniformly impregnated with epoxy resin in vacuum. However, epoxy

*E-mail address: fujishiro@iwate-u.ac.jp

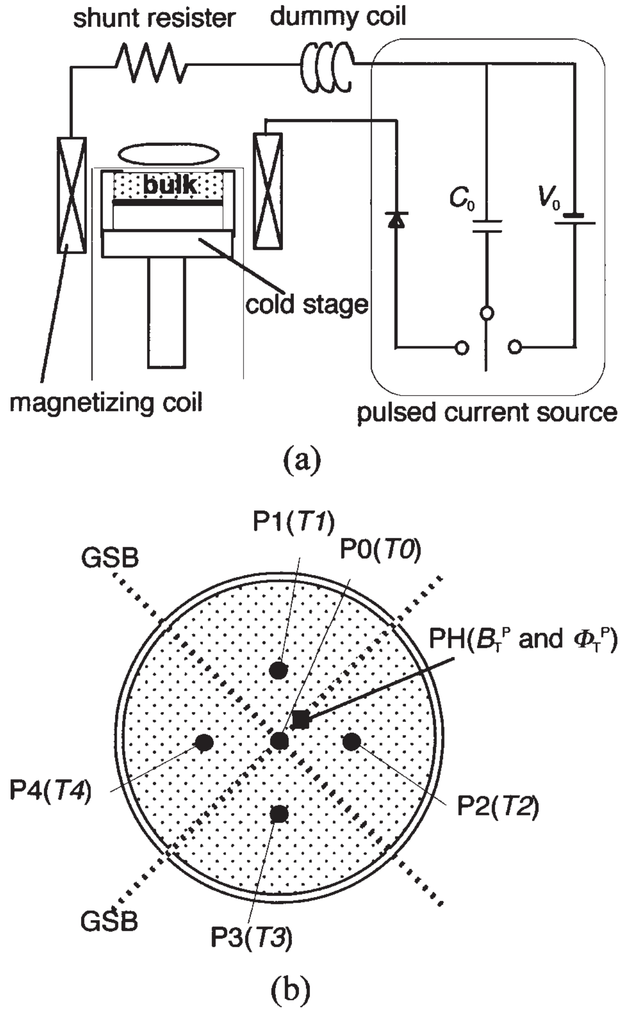

Fig. 1. (a) Experimental setup of the PFM technique. Rise time of the pulse field t_r was changed from 6 to 20 ms by combining the reactance of the dummy coil and/or the capacitance of the condenser bank. (b) Measurement positions of the temperature (P0–P4) and magnetic field (PH) on the bulk.

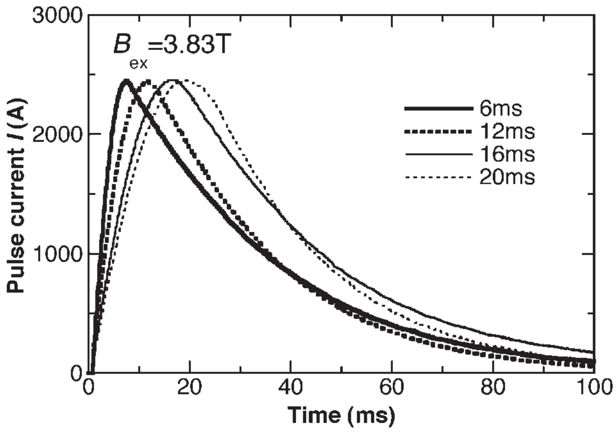

Fig. 2. Examples of the time dependence of current $I(t)$ for each t_r in the case of $B_{ex} = 3.83$ T.

resin on the upper and bottom surfaces was removed to enhance the thermal response. Figure 1(a) shows the experimental setup for the PFM technique. The Sm-bulk was tightly stacked on the sapphire plate on the cold stage of the helium refrigerator in vacuum. The initial stage temperature T_s was held at 40 K. The bulk crystal was magnetized using a pulse magnetization coil ($L = 1.08$ mH, 39 mm in bore radius) dipped in liquid N_2. The rise time of the pulse field t_r was changed from 6 to 20 ms by combining the reactance of a dummy coil ($L = 0$–2.2 mH) and/or the capacitance of the condenser bank ($C_0 = 20$ or 60 mF).

Figure 1(b) shows the positions of the temperature and magnetic field measurements on the bulk. The temperature $T0$ at the bulk center (P0) and the temperatures, $T1$–$T4$, at P1–P4 in the four GSRs were measured using fine chromel-constantan thermocouples (76 μm in diameter) attached to the bulk surface using GE7031 varnish. P1, P2, P3 and P4 were situated at the center of each GSR, 9 mm from P0. Each temperature was recorded about 7 times/s just after applying the pulse field. The Hall sensor (F.W. Bell, model BHA 921) was attached at position PH on the growth sector boundary (GSB) 2.5 mm from P0. The time evolution of the local field $B_L^P(t)$ was monitored using a digital oscilloscope (Yokogawa Electric, DL1640). The time dependence of the applied field $\mu_0 H_a(t)$ was also monitored from the current $I(t)$ flowing in the shunt resistor. The maximum strength of the pulse field $\mu_0 H_a(t)$ was defined as B_{ex}, and it ranged from 3.83 to 5.53 T. Five magnetic pulses (Nos. 1–5) with the same B_{ex} were applied sequentially after recooling to T_s, and $T(t)$ and $B_L^P(t)$ were measured at each stage.

The trapped field B_T^P was also measured at PH using the same Hall sensor. The two-dimensional distribution of the trapped field $B_T^{3\,mm}$ was monitored at each stage using an axial Hall sensor scanned stepwise 3 mm above the bulk surface with a pitch of 1.2 mm. The trapped field B_T^{FC} by FCM was also measured at several temperatures using the cryocooled superconducting magnet. During FCM, the static magnetic field of 5 T was decreased to 0 T in 18 min (0.278 T/min).

Figure 2 shows examples of the time dependence of current $I(t)$ for each t_r in the case of $B_{ex} = 3.83$ T. Each pulse is a maximum at $t_r = 6$–20 ms and then recovers to zero in ~120 ms.

3. Results and Discussion

3.1 Temperature rise and trapped field

Figures 3(a)–3(d) show examples of the time evolutions of $T0(t)$–$T4(t)$ on the bulk after applying the No. 1 and No. 5 pulse fields of (a) $B_{ex} = 3.83$ T with $t_r = 6$ ms, (b) $B_{ex} = 3.83$ T with $t_r = 20$ ms, (c) $B_{ex} = 4.70$ T with $t_r = 6$ ms, and (d) $B_{ex} = 4.70$ T with $t_r = 20$ ms. The distribution of $B_T^{3\,mm}$ for the No. 1 pulse is shown in the inset of each figure. For $B_{ex} = 3.83$ T shown in Figs. 3(a) and 3(b), $T3(t)$ clearly shows a peak with a faster rise for the No. 1 pulse, which suggests that the powerful heat source is located in the vicinity of P3. The magnetic fluxes preferentially intrude into the bulk through the path around P3, where heat generation takes place. The maximum temperature rise ΔT_{max} at $T3$ for $t_r = 20$ ms (= 18 K) is larger than that for $t_r = 6$ ms (= 14 K) and the ΔT values at all the positions increase with increasing t_r. The trapped field $B_T^{3\,mm}$ at the bulk center is always small but $B_T^{3\,mm}$ for $t_r = 20$ ms is larger than that for $t_r = 6$ ms.

For the No. 1 pulse of $B_{ex} = 4.70$ T shown in Figs. 3(c) and 3(d), the temperature rise ΔT at each position increases

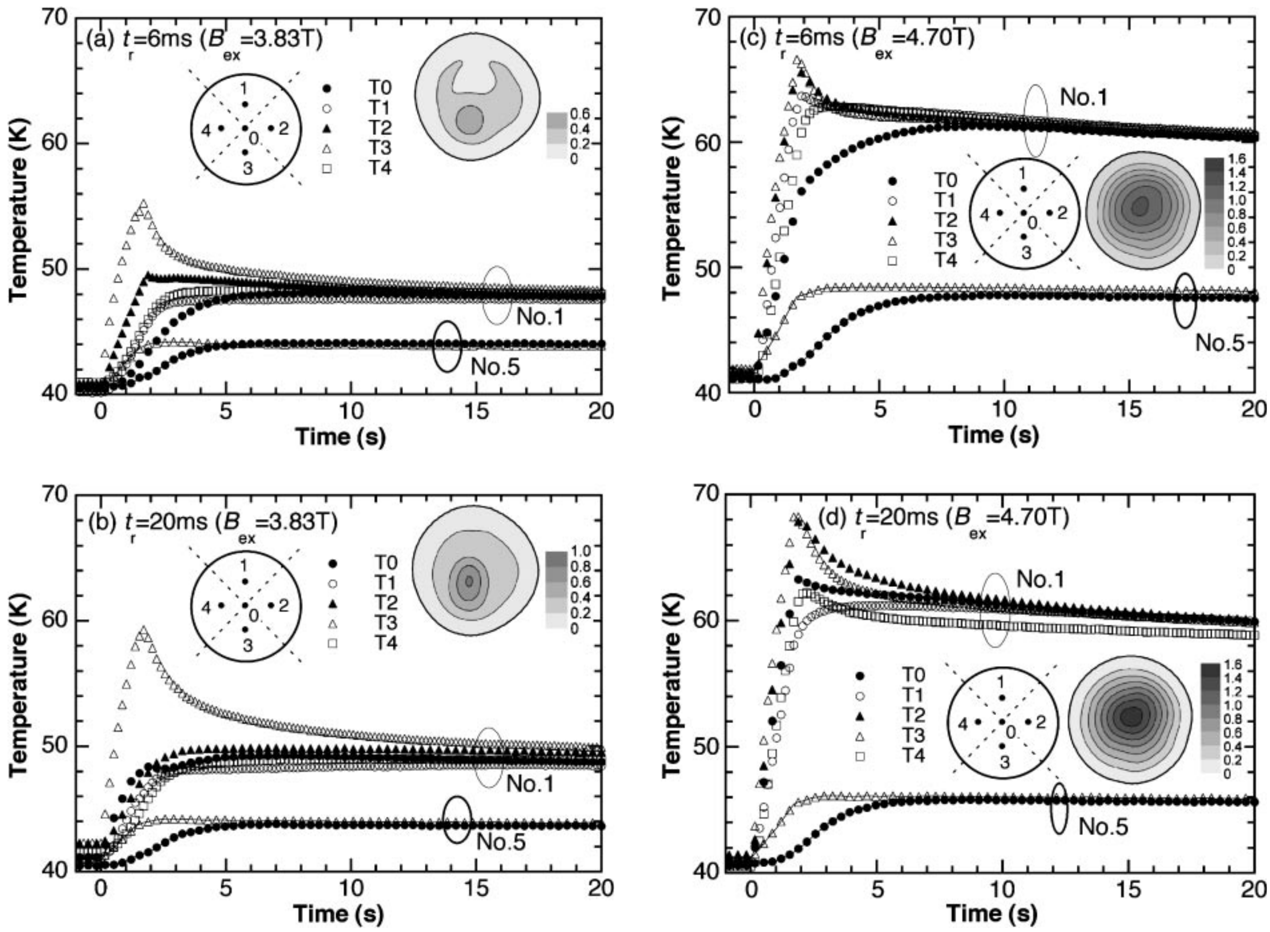

Fig. 3. Time evolutions of temperatures $T0(t)$–$T4(t)$ after applying the No. 1 and No. 5 pulse fields: (a) $t_r = 6$ ms with $B_{ex} = 3.83$ T, (b) $t_r = 20$ ms with $B_{ex} = 3.83$ T, (c) $t_r = 6$ ms with $B_{ex} = 4.70$ T and (d) $t_r = 20$ ms with $B_{ex} = 4.70$ T. For the No. 5 pulse, only $T0(t)$ and $T3(t)$ are shown in each figure.

compared with that for $B_{ex} = 3.83$ T. $T2(t)$ also shows a peak, as does $T3(t)$. $T0(t)$ at the bulk center shows a slower temperature rise for $t_r = 6$ ms, which suggests that the main heat source is far from the bulk center. On the other hand, $T0(t)$ for $t_r = 20$ ms rises faster with a faint peak which suggests that flux motion and heat generation take place also around the center. The distribution of $B_T^{3\,mm}$ in both figures shows a conical shape but the peak value in $B_T^{3\,mm}$ for $t_r = 20$ ms is somewhat larger than that for $t_r = 6$ ms. The temperature rise ΔT decreases with increasing pulse number and shows a tendency to a saturate after the third (No. 3) pulse application. There is no peak in $T(t)$ for the No. 5 pulse, which suggests that flux motion and heat generation take place in all GSRs equally.

Figure 4(a) shows the maximum temperature rise $\Delta T0_{max}$ at P0 for the No. 1 and No. 5 pulses as a function of t_r. For the No. 1 pulse of $B_{ex} = 3.83$ T and 4.70 T, $\Delta T0_{max}$ increases with increasing t_r and with increasing B_{ex}. However, for the No. 1 pulse of $B_{ex} = 5.53$ T, $\Delta T0_{max}$ slightly decreases with increasing t_r. On the other hand, $\Delta T0_{max}$ for the No. 5 pulse, which is far smaller than that for the No. 1 pulse, decreases with increasing t_r particularly for $B_{ex} = 4.70$ T. Figure 4(b) shows the trapped field B_T^P at the position PH as a function of t_r for each B_{ex}. For the No. 1 pulse of $B_{ex} = 3.83$ T, B_T^P increases monotonically with increasing t_r. For $B_{ex} = 4.70$ T, the markedly enhanced B_T^P value further increases and then saturates with increasing t_r. For the No. 1 pulse of $B_{ex} = 5.53$ T, B_T^P decreases with decreasing t_r.

Figure 5 summarizes the relationship between B_T^P and the maximum temperature $T0_{max}$ after applying the No. 1 pulse for various t_r values. Using the data shown in Figs. 4(a) and 4(b), data sets of ($T0_{max}$, B_T^P) are plotted for each B_{ex} and t_r. The measured trapped field $B_T^{FC}(T)$ is also presented, which corresponds to the maximum flux trapping ability of the present SmBaCuO bulk. The data sets of $B_{ex} = 3.83$ and 4.70 T are situated below the B_T^{FC}–$T0_{max}$ line. When $B_{ex} =$ 4.70 T is applied, B_T^P becomes the largest for $t_r = 20$ ms and then decreases with decreasing t_r. On the other hand, for $B_{ex} = 5.53$ T, the B_T^P value becomes the largest for $t_r = 6$ ms and then decreases with increasing t_r. The B_T^P values for $t_r = 12$ and 16 ms are smaller than those for $B_{ex} = 4.70$ T because of the increase of heat generation; $T0_{max}$ touches the B_T^{FC}–$T0_{max}$ line and the B_T^P decrease follows it with the further increase of temperature. The results of these analyses demonstrate that the flux trapping ability by the PFM technique can be systematically explained as being limited by the B_T^{FC}–$T0_{max}$ line.

Figure 6 shows the time evolutions of the applied field $\mu_0 H_a(t)$ and the local field $B_L^P(t)$ at PH for (a) $t_r = 6$ ms with $B_{ex} = 4.70$ T, (b) $t_r = 16$ ms with $B_{ex} = 4.70$ T, (c) $t_r = 6$ ms with $B_{ex} = 5.53$ T and (d) $t_r = 16$ ms with $B_{ex} = 5.53$ T for

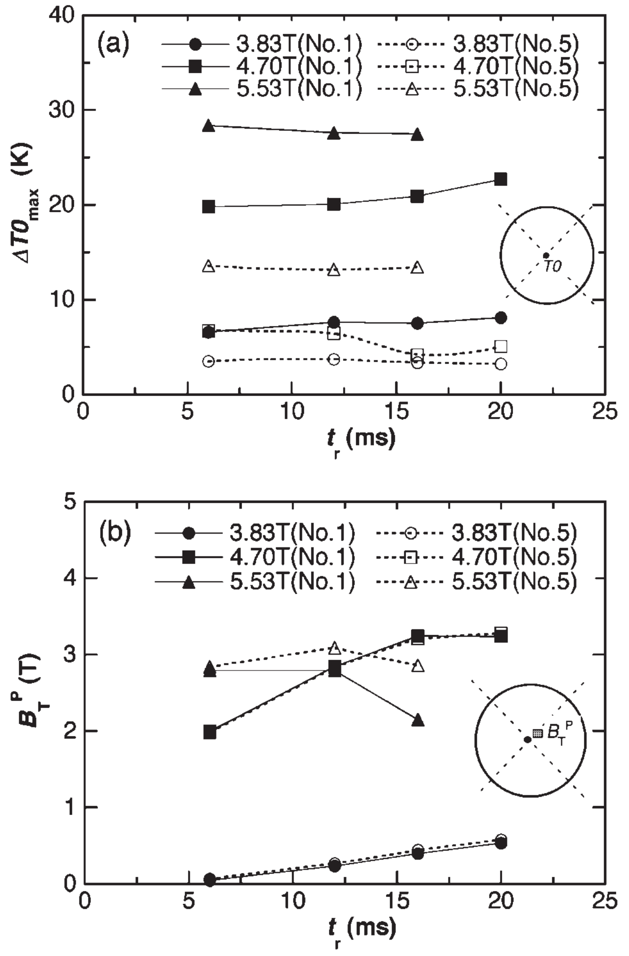

Fig. 4. (a) Maximum temperature rise $\Delta T0_{max}$ at P0 and (b) trapped field B_T^P at PH for the No. 1 and No. 5 pulses as a function of rise time t_r.

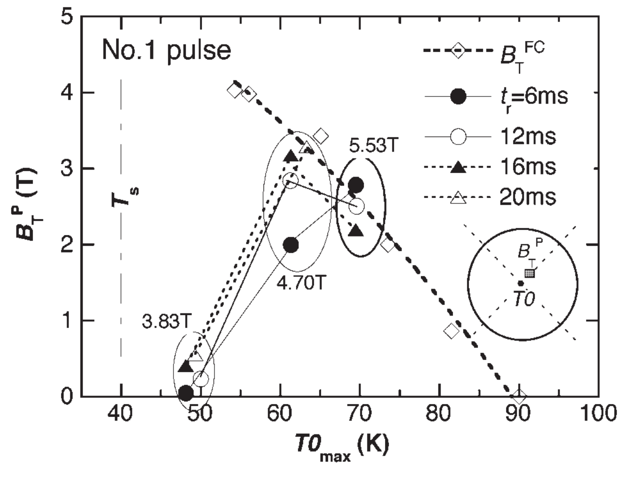

Fig. 5. B_T^P value as a function of maximum temperature $T0_{max}$ for the No. 1 pulse with various t_r.

the No. 1 pulse. In Fig. 6(a) for $t_r = 6$ ms with $B_{ex} = 4.70$ T, the maximum $B_L^P(t)$ is about one-half of B_{ex}. The rise time of $B_L^P(t)$ is about $t_r^B = 6.5$ ms. On the other hand, for $t_r = 16$ ms shown in Fig. 6(b), the rise time of $B_L^P(t)$ increases to about $t_r^B = 9$ ms and the magnetic field of ~4.5 T, which is almost as large as B_{ex}, enters the bulk and then slowly decreases due to flux creep. As a result, the trapped field B_T^P is ultimately reduced to 3.2 T, as shown in Fig. 4(b). Similar behaviors were also confirmed for $B_{ex} = 5.53$ T with $t_r = 6$ ms and 16 ms, as shown in Figs. 6(c) and 6(d), respectively; t_r^B (= 10 ms) for $t_r = 16$ ms is elongated compared with t_r^B (= 6.5 ms) for $t_r = 6$ ms. For $B_{ex} = 5.53$ T with $t_r = 16$ ms, the maximum of the local field attains almost 5.5 T, but this high value of B_L^P causes a more intense flux creep, resulting in a smaller trapped field B_L^P (~2.1 T) than that (~2.8 T) for $t_r = 6$ ms.

In Figs. 6(a)–6(d), we note that the increase of $B_L^P(t)$ starts at about the applied pulse field $\mu_0 H_a(t) \sim 4.3$ T regardless of the maximum pulse field B_{ex} and the rise time t_r. This suggests that the surface barrier against flux penetration breaks down at about 4.3 T in the virgin run. The strength of the surface barrier results from the critical current density J_c of the bulk and is independent of the B_{ex} and t_r values. The existence of the surface barrier of ~4.3 T is consistent with the drastic increase of B_T^P between $B_{ex} = 3.83$ and 4.70 T. In Fig. 6(e), for the No. 5 pulse of $B_{ex} = 4.70$ T, the variation of $B_L^P(t)$ is very small but the response of $B_L^P(t)$ shows no delay against the magnetic pulse. The surface barrier seems to be removed owing to the magnetic flux already trapped in the bulk.

Assuming the relation $v = d/t_r^B$, where d (= 20 mm) is the distance between the bulk edge and the position PH, the flux velocity v is roughly estimated to be 3.1 m/s for $t_r = 6$ ms and 2.2 m/s for $t_r = 16$ ms, which are reasonable values compared with those determined by the pick-up coil technique.[6)] It should be noted that the propagation speed v of magnetic flux in the bulk only modestly changes in contrast to the large change of t_r. In the following subsection, we estimate the total generated heat Q and separate the pinning loss Q_p and the viscous loss Q_v from the total Q.

3.2 Estimation of generated heat Q

If we assume that the heat generation occurs during PFM under the adiabatic condition, the total generated heat Q, which is the sum of Q_p and Q_v, is given by[10)]

$$Q = \int_{T_s}^{T_s+\Delta T_{max}} C(T)V\,dT = Q_p + Q_v \qquad (3.1)$$

where $C(T)$ is the specific heat and V is the volume of the bulk disk. $C(T)$ was estimated using the relation $C = \kappa/\alpha$, i.e., the thermal conductivity κ divided by the thermal diffusivity α, which were measured simultaneously.[14)] Figure 7 presents the estimated Q(No. 1) and Q(No. 5) values after the No. 1 and No. 5 pulses and the difference dQ [= Q(No. 1) − Q(No. 5)] for $B_{ex} = 4.70$ T as a function of t_r. Since no additional flux trapping takes place with the No. 5 pulse, as described in the previous paper,[12)] Q(No. 5) may consist mainly of viscous loss Q_v and dQ can be roughly regarded as the pinning loss Q_p for the No. 1 pulse. In Fig. 7, Q(No. 1) and dQ increase with increasing t_r. On the other hand, it should be noted that Q(No. 5) decreases with increasing t_r. The decrease of v for longer t_r may be mainly responsible for the decrease of Q(No. 5) ($\simeq Q_v$) because Q_v is proportional to v.

The magnetization M at PH can be estimated from the $\mu_0 H_a(t)$ and $B_L^P(t)$ values using

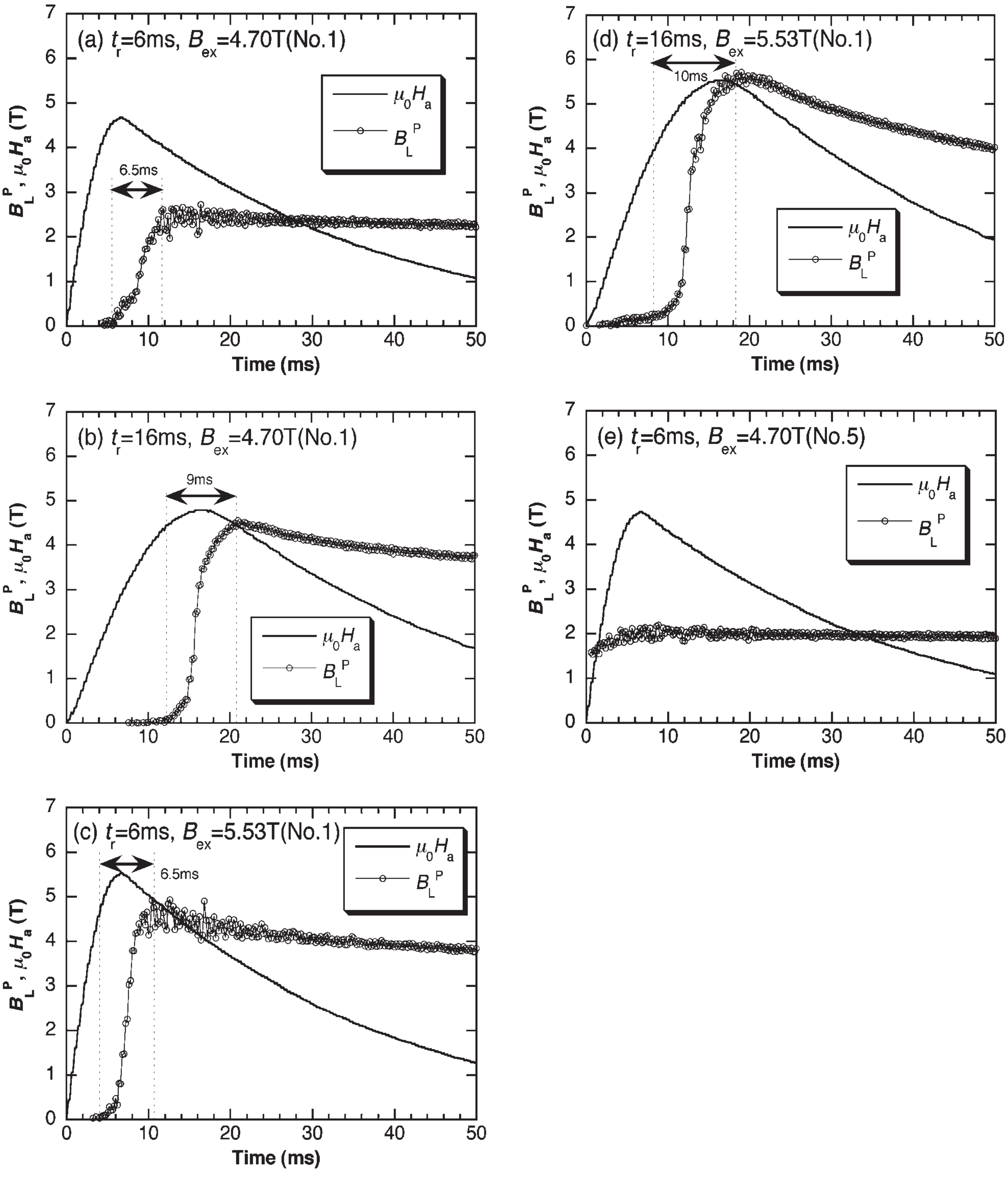

Fig. 6. Time evolutions of the applied field $\mu_0H_a(t)$ and local field $B_L^P(t)$ for (a) $t_r = 6$ ms with $B_{ex} = 4.70$ T, (b) $t_r = 16$ ms with $B_{ex} = 4.70$ T, (c) $t_r = 6$ ms with $B_{ex} = 5.53$ T and (d) $t_r = 16$ ms with $B_{ex} = 5.53$ T for the No. 1 pulse. (e) Time evolution of $\mu_0H_a(t)$ and $B_L^P(t)$ upon applying the No. 5 pulse of $t_r = 6$ ms with $B_{ex} = 4.70$ T.

$$M = B_T^P - \mu_0H_a. \tag{3.2}$$

Figure 8(a) shows the M vs μ_0H_a curves for the No. 1 pulse of $B_{ex} = 4.70$ T with $t_r = 6$ ms, 12 ms and 16 ms. Following the critical state model, the pinning loss $Q_p(MH)$ can be obtained from the area of the M–μ_0H_a hysteresis loop. A wide hysteresis loop in the M–μ_0H_a curve can be clearly seen for each t_r, which results from flux trapping in the bulk disk. The area of the hysteresis loop is enhanced with increasing t_r, corresponding to the enhancement of B_T^P in Fig. 4(b). Figure 8(b) presents the pulse number dependence of the M vs μ_0H_a curves for $t_r = 12$ ms with $B_{ex} = 4.70$ T. The hysteresis loop becomes drastically narrow for the No. 2 pulse and no hysteresis behavior can be observed for the No. 5 pulse. These behaviors are consistent with the pulse number dependences of B_T^P and support the hysteresis loop being directly related to flux trapping.[12] The $Q_p(MH)$ values estimated from the area of the hysteresis loop are also plotted in Fig. 7. It should be noted that the $Q_p(MH)$ values are nearly equal to dQ determined from the temperature

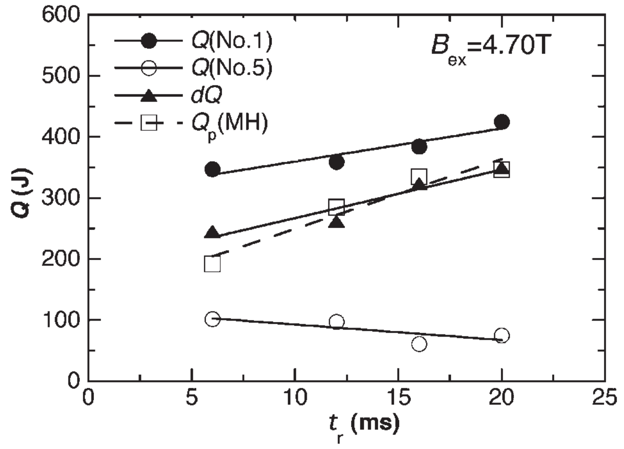

Fig. 7. Estimated Q(No. 1) and Q(No. 5) values after the No. 1 and No. 5 pulses and the difference dQ [$= Q$(No. 1) $- Q$(No. 5)] for $B_{ex} = 4.70$ T as a function of t_r. The $Q_p(MH)$ values estimated from the M–$\mu_0 H_a$ hysteresis loop [in Fig. 8(a)] are also plotted.

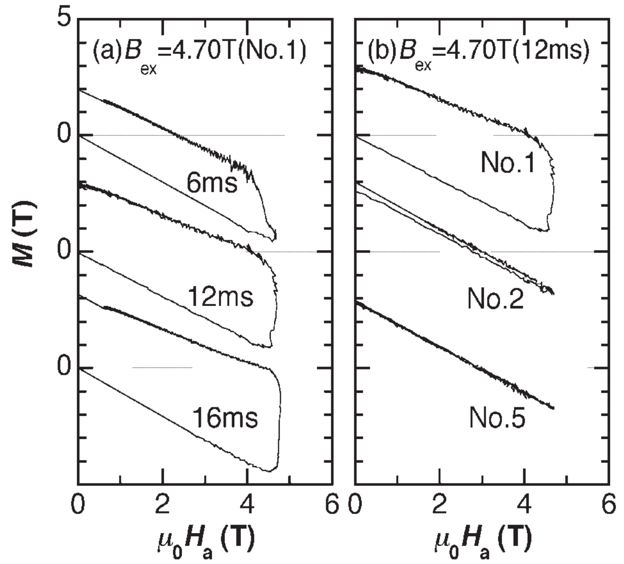

Fig. 8. (a) M vs $\mu_0 H_a$ curves for $t_r = 6$, 12 and 16 ms with $B_{ex} = 4.70$ T for the No. 1 pulse. (b) Pulse number dependence of M vs $\mu_0 H_a$ curves for $B_{ex} = 4.70$ T with $t_r = 12$ ms.

measurement. These results suggest the validity of estimating pinning loss from the measured temperature. Thus the viscous loss Q_v can be reliably estimated on the basis of the Q(No. 5) value.

4. Summary

The rise-time elongation effect of the magnetic pulse ($B_{ex} = 3.83$–5.53 T) on the temperature rise ΔT and the trapped field B_T^P has been investigated for various rise times t_r ($= 6$–20 ms) for the cryocooled SmBaCuO bulk superconductor. Main experimental results and conclusions obtained in this study are summarized as follows.

(1) Under identical magnetic pulse strengths B_{ex}, the temperature rise ΔT and the trapped field B_T^P change depending on the rise time t_r of the magnetic pulse.

(2) For $B_{ex} \leq 4.70$ T, ΔT and B_T^P increase with increasing t_r. On the other hand, for $B_{ex} = 5.53$ T, ΔT and B_T^P decrease with increasing t_r. The reduction of B_T^P takes place because of the large ΔT. These results can be systematically explained on the basis of the diagram of the trapped field induced by the field-cooled magnetization (FCM) B_T^{FC} vs maximum temperature $T0_{max}$.

(3) The B_T^P value for the virgin-state bulk is governed not only by the pulse field strength B_{ex} but also by the rise time t_r. The maximum B_T^P can be achieved with the optimum combination of B_{ex} and t_r. In other word, there is a characteristic B_{ex} for each t_r which maximizes the B_T^P value.

(4) In the present SmBaCuO bulk in the virgin state, there exists a surface barrier against flux penetration, but it is destroyed by the applied magnetic pulse of ~4.3 T. For the following pulse field application, the barrier is eliminated by the previously trapped flux.

(5) The five pulse fields (Nos. 1–5) with the fixed strength B_{ex} were applied to the bulk and the generated heat Q was estimated using the maximum temperature rise $\Delta T0_{max}$ and the specific heat C. Heat generation Q(No. 5) after the No. 5 pulse, which is mainly contributed by the viscous loss Q_v, decreases with increasing t_r. The t_r dependence of Q(No. 5) may mainly result from the decrease of the flux propagation velocity v, which was confirmed from the time dependence of the local field $B_L^P(t)$ at position PH in the bulk. The dQ [$= Q$(No. 1) $- Q$(No. 5)] value, which is regarded as the pinning loss Q_p for the No. 1 pulse, increases with increasing t_r for $B_{ex} = 4.70$ T, in accord with the observed t_r dependence of B_T^P.

(6) The pinning loss $Q_p(MH)$ was estimated from the hysteresis loop of the magnetization M vs the applied field $\mu_0 H_a$. The $Q_p(MH)$ value is nearly equal to dQ estimated from the measured temperature. This result is consistent with our assumption that dQ can be regarded as the pinning loss and that the viscous loss Q_v can be given by Q(No. 5).

Acknowledgements

The valuable suggestions by Professor M. Ikebe of Iwate University are greatly acknowledged. This work is partially supported by Japan Science and Technology Agency under the Joint-Research Project for Regional Entities in Iwate Prefecture on development of practical applications of magnetic field technology for use in the region and in everyday living.

1) H. Hayashi, K. Tsutsumi, N. Saho, N. Nishijima and K. Asano: Physica C **392–396** (2003) 745.
2) U. Mizutani, H. Hazama, T. Matsuda, Y. Yanagi, Y. Itoh, K. Sakurai and A. Imai: Supercond. Sci. Technol. **16** (2003) 1207.
3) U. Mizutani, T. Oka, Y. Itoh, Y. Yanagi, M. Yoshikawa and H. Ikuta: Appl. Supercond. **6** (1998) 235.
4) M. Sander, U. Sutter, R. Koch and M. Klaser: Supercond. Sci. Technol. **13** (2000) 841.
5) H. Fujishiro, K. Yokoyama, M. Kaneyama, T. Oka and K. Noto: to be publihed in IEEE Trans. Appl. Supercond. (2005).
6) Y. Yanagi, Y. Itoh, M. Yoshikawa, T. Oka, A. Mase, T. Hosokawa, H. Ikuta and U. Mizutani: *Advances in Superconductivity X* (Springer, Tokyo, 1998) p. 717.
7) A. Terasaki, Y. Yanagi, Y. Itoh, M. Yoshikawa, T. Oka, H. Ikuta and U. Mizutani: *Advances in Superconductivity X* (Springer, Tokyo, 1998) p. 945.
8) Y. Itoh, Y. Yanagi and U. Mizutani: J. Appl. Phys. **82** (1997) 5600.

9) H. Fujishiro, T. Oka, K. Yokoyama and K. Noto: Supercond. Sci. Technol. **16** (2003) 809.
10) H. Fujishiro, M. Kaneyama, K. Yokoyama, T. Oka and K. Noto: Supercond. Sci. Technol. **18** (2005) 158.
11) H. Fujishiro, T. Oka, K. Yokoyama and K. Noto: Supercond. Sci. Technol. **17** (2004) 57.
12) H. Fujishiro, T. Oka, K. Yokoyama, M. Kaneyama and K. Noto: IEEE Appl. Supercond. **14** (2004) 1054.
13) H. Fujishiro, K. Yokoyama, M. Kaneyama, M. Ikebe, T. Oka and K. Noto: to be published in Physica C (2005).
14) H. Fujishiro and S. Kohayashi: IEEE Trans. Appl. Supercond. **12** (2002) 1124.